Journal of Environmental Chemical Engineering 10 (2022) 107799

Contents lists available at ScienceDirect

Journal of Environmental Chemical Engineering

journal homepage: www.elsevier.com/locate/jece

Syntrophy drives the microbial electrochemical oxidation of toluene in a continuous-flow "bioelectric well"

Matteo Tucci [a], Alessandro Milani [a], Marco Resitano [a], Carolina Cruz Viggi [a], Ottavia Giampaoli [b], Alfredo Miccheli [c], Simona Crognale [a], Bruna Matturro [a], Simona Rossetti [a], Falk Harnisch [d], Federico Aulenta [a,*]

[a] Water Research Institute (IRSA), National Research Council (CNR), 00015 Monterotondo, RM, Italy
[b] NMR-based Metabolomics Laboratory (NMLab), Department of Chemistry, Sapienza University of Rome, RM, Italy
[c] NMR-based Metabolomics Laboratory (NMLab), Department of Environmental Biology, Sapienza University of Rome, RM, Italy
[d] Department of Environmental Microbiology, Helmholtz Centre for Environmental Research GmbH - UFZ, Permoserstraße 15, Leipzig 04318, Germany

ARTICLE INFO

Editor: Yang Liu

Keywords:
Microbial electrochemical technologies
Groundwater remediation
Bioremediation
Toluene
Petroleum hydrocarbons

ABSTRACT

Microbial electrochemical technologies (MET) are promising for the remediation of groundwater pollutants such as petroleum hydrocarbons (PH). Indeed, MET can provide virtually inexhaustible electron donors or acceptors directly in the subsurface environment. However, the degradation mechanisms linking contaminants removal to electric current flow are still largely unknown, hindering the development of robust design criteria.

Here, we analysed the degradation of toluene, a model PH, in a bioelectrochemical reactor known as "bioelectric well" operated in continuous-flow mode at various influent toluene concentrations. With increasing concentration of toluene, the removal rate increased while the current tended to a plateau, hence the columbic efficiency decreased. Operation at open circuit confirmed that the bioelectrochemical degradation of toluene proceeded via a syntrophic pathway involving cooperation between different microbial populations. First of all, hydrocarbon degraders quickly converted toluene into metabolic intermediates probably by breaking the aromatic ring upon fumarate addition. Subsequently, fermentative bacteria converted these intermediates into volatile fatty acids (VFA) and likely also H_2, which were then used as substrates by electroactive microorganisms forming the anodic biofilm. As toluene degradation is faster than subsequent conversion steps, the increase in intermediate concentration could not result in a current increase.

This work provides valuable insights on the syntrophic degradation of BTEX, which are essential for the application of microbial electrochemical system to groundwater remediation of petroleum hydrocarbons.

1. Introduction

The presence of petroleum hydrocarbons (PHs) in groundwater is mostly caused by accidental spills and industrial discharges, and it represents a critical threat to human health and the ecosystem [50]. Due to their high mobility and water solubility, benzene, toluene, ethylbenzene and xylenes (BTEX) are particularly dangerous when dispersed in the environment [1], often amounting up to 90% of the dissolved pollutants in groundwater contamination plumes [43]. This aspect, combined with the toxicity, demands for the implementation of effective remediation strategies [3].

In this regard, bioremediation is considered an effective strategy: it takes advantage of the capability of naturally occurring microorganism to use pollutants as substrates and convert them into harmless or less dangerous products [30]. In subsurface environments, however, bioremediation is often limited by the scarcity of bioavailable electron acceptors or donors, negatively affecting the removal rates [28]. To overcome this problem, several remediation techniques have emerged, which mainly involve the injection of soluble electron acceptors (*e.g.* oxygen) or donors (e.g. lactate) into the contaminated aquifer to enhance the metabolism of the degrading microbial communities [11]. Microbial electrochemical technologies (METs) are emerging as a viable alternative to this approach, by supplying a virtually inexhaustible electron acceptor or donor directly in the subsurface environment in the form of a solid electrode [6,46]. In this way, several drawbacks linked to traditional bioremediation strategies can be avoided, such as: (a) quick

* Corresponding author.
E-mail address: federico.aulenta@irsa.cnr.it (F. Aulenta).

https://doi.org/10.1016/j.jece.2022.107799
Received 7 March 2022; Received in revised form 15 April 2022; Accepted 23 April 2022
Available online 27 April 2022

consumption or migration of the amendment solution; (b) contaminant plume shift or dilution caused by the injection; (c) uncontrolled biomass growth near injection points and (d) accumulation of unwanted metabolites derived from the amendment [17]. For this reason, METs can result in a more sustainable and cost-effective technology. However, only few studies have addressed the use METs for the anaerobic oxidation of BTEX [53], and in order to design effective prototypes for field applications, a deeper understanding of the removal mechanisms is necessary.

Herein, we studied the degradation of toluene as model BTEX using a prototype of MET called "bioelectric well". In previous works this prototype has been successfully tested for the removal of phenol, toluene or a mixture of BTEX in continuous-flow mode [31–33,47]. It consists of a membrane-less tubular bioelectrochemical reactor where anode and cathode are placed concentrically and in close proximity to each other in order to minimize ohmic losses. Importantly, due to the cylindrical shape and close inter-electrode spacing even upon scale-up, the bioelectric well could be directly installed inside groundwater wells or piezometers for in-situ treatment of PH. In this work we analyzed the performances of the system in several operational conditions, such as different contaminant loads, open circuit vs. polarized, continuous-flow mode vs. batch mode, etc., in order to identify the main factors that influence the degradation process and its possible limitations. Furthermore, we monitored the concentration of metabolites in the liquid phase of the reactor and conducted microbiological analyses to have a deeper understanding of the microbial interactions responsible for degradation of toluene.

2. Materials and methods

2.1. Chemicals and electrode potentials

All chemicals were of analytical grade and were supplied from Merck KGaA (Darmstadt, Germany). De-ionized water (Millipore, Darmstadt, Germany) was used to prepare the microbial medium, and all other solutions. All potentials provided in this article refer to the standard hydrogen electrode (SHE).

2.2. Reactor setup and operations

The bioelectric well was constructed as described elsewhere [47]. A cylindrical anode made of 8 contiguous graphite rods (purity: 99.995%, length: 30 cm, ø: 0.6 cm; Sigma-Aldrich, Italy) and a stainless-steel mesh cathode (dimensions: 3 × 30 cm; type 304, Alpha Aesar, USA) were concentrically placed in a 250 mL glass cylinder (Fig. S1). Anode and cathode were kept physically separated by a polyethylene mesh (ø: 1 cm, length 30 cm; Fig. 1B), which still allowed hydraulic connection. Titanium wires (ø: 0.81 mm Alfa Aesar, USA) were used to connect anode and cathode to an external circuit. The anode was continuously polarized at + 0.2 V vs. SHE by an IVIUMnSTAT potentiostat (IVIUM Technologies, The Netherlands), and an Ag/AgCl electrode (+0.198 V vs. SHE; AMEL, Italy) was used as reference electrode.

The inoculum consisted of 0.25 L of contaminated groundwater obtained from a petrochemical site in Italy. The reactor was continuously fed with mineral medium (Tab. S1). Prior to use, the medium inlet was sparged with pure nitrogen gas to eliminate oxygen. Then the medium was spiked with toluene at a different concentration for each feeding cycle, ranging from about 1–40 mg L^{-1} (Table 1). The inlet was then stored in 5 L collapsible Tedlar® gas bags. The medium was pumped into the reactor through a port situated at the bottom of the cylinder (flow rate: 0.63 L d^{-1}, HRT 11 h) using a peristaltic pump (120S, Watson Marlow, Falmouth, UK), while the treated effluent exited from a port near the upper end by passive overflow. The inlet and at the outlet of the reactor were equipped with flow-through sampling cells (volume: 25 mL). In order to avoid the formation of concentration gradients of substrate, products and biomass, the liquid phase of the reactor was constantly recycled with another peristaltic pump (flow rate: 192 mL min^{-1}; model: 323, Watson Marlow, Falmouth, UK; Fig. S1). All the tubings were made of Viton® (Sigma-Aldrich, Italy), which keeps volatilization losses and organic contaminant adsorption to a minimum. At the end of the experiment the electrodes were disconnected from the potentiostat and the reactor was operated at open circuit potential (OCP) as a control condition. Furthermore, in a follow-up experiment the reactor was operated in OCP and in batch mode to analyze the possible accumulation of degradation intermediates. Throughout the

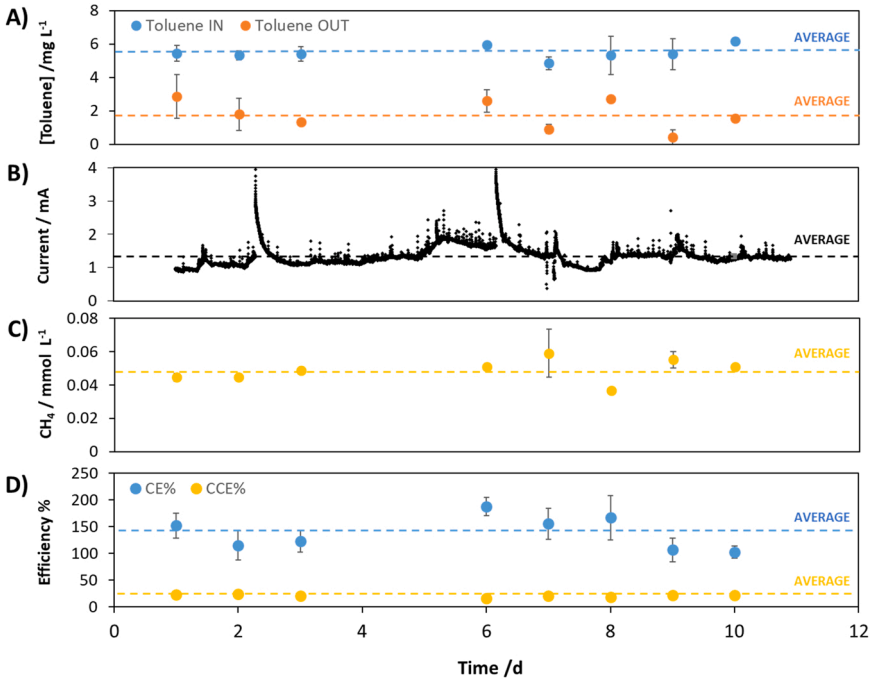

Fig. 1. Trends of A) toluene concentrations in the influent and effluent of the reactor, B) current generation, C) methane produced, D) coulombic efficiency (CE) and cathode capture efficiency (CCE) for the third experimental run of the reactor (Inlet toluene concentration 5.5 mg L^{-1}).

Table 1
Average values of performance indicators during each experimental run (see calculation section).

Run	Duration (d)	Tol_{in} (mg L^{-1})	Tol_{out} (mg L^{-1})	r_{Tol} (mg L^{-1} d^{-1})	q_{Tol} (%)	Current (mA)	Met_{out} (mmol L^{-1})	*CE* (%)	*CCE* (%)
I	8	17.0 ± 1.6	3.9 ± 0.3	28 ± 3	76 ± 3	1.86 ± 0.04	0.18 ± 0.02	55 ± 7	56 ± 5
II	8	23.7 ± 2.9	10.4 ± 1.6	29 ± 4	56 ± 3	1.94 ± 0.03	0.10 ± 0.01	56 ± 7	30 ± 3
III	15	5.5 ± 0.1	1.8 ± 0.3	8 ± 1	68 ± 6	1.33 ± 0.09	0.049 ± 0.002	134 ± 10	21 ± 1
IV	9	9.0 ± 1.2	4.0 ± 0.4	11 ± 2	55 ± 3	1.58 ± 0.06	0.06 ± 0.01	123.1 ± 0.2	23 ± 5
V	7	0.9 ± 0.7	0.2 ± 0.1	2 ± 1	76 ± 7	1.06 ± 0.07	0.03 ± 0.02	2275 ± 753	11 ± 6
VI	4	39.7 ± 8.8	7.1 ± 3.4	71 ± 13	85 ± 5	2.44 ± 0.45	0.03 ± 0.01	30 ± 9	8 ± 1
OCP	8	26.4 ± 0.6	10.5 ± 1.0	35 ± 3	60 ± 5	/	0.06 ± 0.01	/	/

whole study, the system was kept at room temperature (i.e., 24 ± 3 °C).

2.3. Cyclic voltammetries

Cyclic voltammetries (CVs) were conducted on the bioanode at scan rates of 1 mV/s within the potential range between − 0.4 and 0.8 V vs. SHE using an IVIUMnSTAT potentiostat (IVIUM Technologies, The Netherlands). The stainless-steel cathode was used as counter electrode, while an Ag/AgCl electrode (+0.198 V vs. SHE; AMEL, Italy) served as reference.

2.4. Gas analyses

Gaseous samples were analyzed in terms of O_2, H_2 and CH_4 using a gas-chromatograph (Agilent 8860, GC system USA) equipped with a thermal conductivity detector (TCD). The concentration of toluene was measured by injecting gaseous samples into a gas-chromatograph (Agilent 8860, GC system USA) equipped with a flame ionization detector (FID). Gas-phase concentrations were converted into liquid-phase concentrations using tabulated Henry's Law constants [39]. The GC methods, calibration ranges and LOD of analytical methods are reported in the Supporting Information (Tab S2).

2.5. ^1H NMR analyses of liquid samples

The liquid samples collected during the batch phase operated in OCP mode were analyzed via Proton Nuclear Magnetic Resonance (^1H NMR) spectroscopy. Initially, 350 microliters of each sample were added to 350 microliters of trimethylsilyl propionic-2,2,3,3-d4 acid (TSP)- D2O 2 mM solution (final concentration of 1 mM). This mixture of each sample was then vortexed and transferred into precision tubes. After that, 1H NMR spectra were acquired at 298 K using a JEOL JNM-ECZR spectrometer (JEOL Ltd, Tokyo, Japan) equipped with a magnet operating at 14.09 Tesla and at 600.17 MHz for 1H frequency. All the spectra were recorded with 64k points and 128 scans, setting spectral width to 9.03 KHz (15 ppm), with and irradiation attenuator of 48 dB, a presaturation pulse length of 2.00 s, relaxation delay of 5.72 s, for an acquisition time of 5.81 s. The identification step was achieved by two-dimensional experiments 1–1H Homonuclear Total Correlation Spectroscopy (TOCSY), 1H-13C Heteronuclear Single Quantum Correlation (HSQC) on selected samples and confirmed by literature comparison. TOCSY experiments were recorded at 298 K with a spectral width of 15 ppm in both dimensions, using 8k ×256 data points matrix, repetition time of 3.00 s and 80 scans, with a mixing time of 80.00 ms. HSQC experiments were acquired with a spectral width of 9.03 KHz (15 ppm) in proton dimension and 30 KHz (200 ppm) in the carbon dimension, using 8k × 256 data points matrix for the proton and the carbon dimensions, respectively, with a repetition delay of 2 s and 96 scans. One-dimensional NMR spectra were processed and quantified by using the ACD Lab ^1D NMR Manager ver. 12.0 software (Advanced Chemistry Development, Inc., Toronto, ON, Canada); 2D NMR spectra were processed by using JEOL Delta v5.3.1 software (JEOL Ltd, Tokyo, Japan). All the NMR spectra were manually phased, baseline corrected and referenced to the chemical shift of the TSP methyl resonance at $\delta = 0.00$. The quantification of metabolites was obtained by comparing the integrals of their diagnostic resonances with the internal standard TSP integral and normalized for their number of protons, and then multiplied for two, in order to consider the dilution factor. Final concentration was expressed as mM.

2.6. High-throughput rRNA gene sequencing and bioinformatic analysis

The contaminated groundwater used to inoculate the reactor (T_0: 45 mL) and liquid sample (T_f: 10 mL) taken at the end of the operation were filtered through polycarbonate membranes (pore size 0.2 mm, 47 mm diameter, Nuclepore) and immediately stored at − 20 °C. In addition, the biofilm grown on the graphite rods was also collected at the end of the operation for subsequent microbiological analyses. The DNeasy PowerSoil Pro Kit (QIAGEN - Germantown, MD) was used for the DNA extraction. The genomic DNA was utilized as template for the amplification of the V1-V3 region of 16S rRNA gene of *Bacteria* (27F 5′-AGAGTTTGATCCTGGCTCAG-3′; 534R 5′-ATTACCGCGGCTGCTGG-3′) and the region V3–V5 of 16S rRNA gene of *Archaea* (340F 5′-CCCTAHGGGGYGCASCA-3′; 915R 5′-GWGCYCCCCCGYCAATTC-3′) following the procedure for library preparation and sequencing described in [9]. The samples were paired end sequenced (2×301bp) on a MiSeq platform (Illumina) using a MiSeq Reagent kit v3, 600 cycles (Illumina, USA) following the standard guidelines for preparing and loading samples. Phix control library was spiked at a concentration of 20%.

Bioinformatics elaborations were performed using QIIME2 v. 2018.2 [5] following the procedure reported elsewhere [8]. High-throughput sequencing of the V1-V3 and V3-V5 regions of the bacterial and archaeal 16S rRNA gene yielded a total of 32,274 and 60,744 sequence reads after quality control and bioinformatic processing that resolved into 579 and 81 ASVs, respectively. Dataset are available through the Sequence Read Archive (SRA) under accession PRJNA785770. Sequencing results were used for the calculation of biodiversity indices for each sample (Shannon, Simpson) by using PAST software (PALAEONTOLOGICAL STATISTICS, ver. 2.17) [16].

2.7. Droplet digital PCR quantification of key-functional genes

The QX200™ Droplet Digital™ PCR System (Bio-Rad, Pleasanton, CA) was used in order to quantify the functional genes involved in anaerobic degradation of petroleum hydrocarbons. The ddPCR reaction mixture consisted of 11 μL of 2 × ddPCR EvaGreen supermix (Bio-Rad, Italy), 1 μL of each primer (at 7.5 μM concentration), 6 μL of nuclease-free water, and 3 μL of sample DNA. The reaction mixture was mixed with droplet generation oil (20 μL mixture + 70 μL oil) via microfluidics in the Droplet Generator (Bio-Rad, Italy). Following droplet generation, the water-in-oil droplets were transferred to a standard 96-well PCR plate, which was heat sealed with foil plate seal (Bio-Rad) and placed on a Bio-Rad CFX96 thermocycler (ramping speed at 2 °C s^{-1}) for PCR amplification using the following conditions: 5 min at 95 °C, followed by 39 cycles of 30 s at 95 °C and 1 min at 55–60 °C according to the primer pair, followed by 5 min hold at 4 °C and 5 min at 95 °C. Upon completion of PCR, the plate was transferred to a Droplet Reader (Bio-

Rad) for automatic measurement of fluorescence in each droplet in each well (approximately 2 min per well).

The benzylsuccinate synthase (bssA), involved in toluene degradation, was targeted using 7772 f – 8546r primer pair [51]. The primer pairs bcrCf-bcrCr and bzdNf-bzdnR were used for the amplification of the benzoyl CoA reductases class I (bcrC, bzdN) [21]; while the benzoyl CoA reductase class II (bamB) was amplified using bamBf – bamBr primers [25].

3. Calculations

The removal rate of toluene r (mg L^{-1} d^{-1}) was calculated using the following equation:

$$r_{Tol} = \frac{\Delta Tol}{V_r} \quad Q \tag{1}$$

where ΔTol (mg L^{-1}) is the difference between the concentration of toluene measured in the influent (Tol_{In}) and the concentration measured in the effluent (Tol_{out}), V_r (L) is the empty volume of the reactor and Q (L d^{-1}) is the flow rate of the influent.

The relative toluene removal $q_{Tol\%}$ was calculated as follows:

$$q_{Tol\%} = \frac{\Delta Tol}{C_{Tol(in)}} \times 100 \tag{2}$$

To calculate electron equivalents per day (mmol d^{-1}) generated by the complete oxidation of toluene (meq_{Tol}), the following equation was used:

$$meq_{Tol} \quad = \frac{\Delta Tol}{MW_{Tol}} \times f_{Tol} \times Q \tag{3}$$

where MW_{Tol} is the toluene molecular weight (92.14 g mol^{-1}) and f_{Tol} represents the number of mmol of electrons released from the complete oxidation of 1 mmol of toluene according to the following stoichiometric equation:

$$C_7H_8 + 14H_2O \rightarrow 7\ CO_2 + 36H^+ + 36\ e^- \tag{4}$$

Therefore, the value of f_{Tol} is 36.

Analogously, the electron equivalents per day (mmol d^{-1}) needed for methane production (meq_{Met}) were calculated using the following equation:

$$meq_{Met} \quad = \quad Met_{Out} \times f_{Met} \times Q \tag{5}$$

Where Met_{Out} (mmol L^{-1}) is the concentration of methane measured at in the effluent and f_{Met} represents the number of mmol of electrons necessary for the conversion of 1 mmol of CO_2 to methane, according to Eq. (6), which is equal to 8.

$$CO_2 + 8H^+ + 8\ e^- \rightarrow CH_4 + 2H_2O \tag{6}$$

The columbic efficiency (*CE*) was calculated as the ratio between charge that is the integral of the electric current over time and the theoretical charge deriving from the oxidation of removed toluene, according to the following equation:

$$CE(\%) = \frac{\int i(t) \times dt \quad \times 60 \times 60 \times 24}{(meq_{Tol}) \times F} \quad \times 100 \tag{7}$$

where i is the measured current (mA), dt is the time (s), F is the Faraday's constant (96,485.3 C mol^{-1}), meq_{Tol} is the amount of electron equivalents of toluene removed per day (mmol d^{-1}).

The cathode capture efficiency (*CCE*) of the methane generation was calculated as follows:

$$CCE(\%) = \frac{(meq_{Met}) \times F}{\int i(t) \times dt \quad \times 60 \times 60 \times 24} \quad \times 100 \tag{8}$$

where meq_{Met} represents the millimoles of electron equivalents needed for the production of methane.

The specific (electric) energy consumption (*sEC*, kWh mM^{-1}) was calculated, for each run, from the average value of the electric current (i, A), the measured cell voltage (V), and the average toluene removal rate (r_{Tol}, mg L^{-1} d^{-1}), according to the following equation:

$$sEC \quad (kWh \quad mM^{-1}) = \frac{i \times V}{3600 \times 1000} \quad \frac{MW_{Tol} \times 24 \times 60 \times 60}{r_{Tol}} \tag{9}$$

4. Results and discussion

4.1. Reactor performance

The bioelectric well was operated in continuous-flow mode for about 50 days, and six different runs were performed at different influent toluene concentrations. For each run, current, concentration of toluene in the influent and effluent and methane generation were measured. Moreover, the coulombic efficiency (*CE*) and the cathode capture efficiency (*CCE*) were calculated. Fig. 1 exemplifies the calculation (cycle III, influent toluene concentration: 5.5 ± 1 mg L^{-1}) and the average values for all experimental runs are reported in Table 1.

The highest achieved toluene removal rate (r_{Tol}) was 71 ± 13 mg L^{-1} d^{-1}, with an average degradation of the influent contaminant load of about 70%. The corresponding specific (electric) energy consumption was 6.8 × 10^{-5} kW h mM^{-1}, a value which compares favorably with those reported for other (ground)water treatment processes, particularly advanced oxidation processes (AOPs) [27].

The *CE* was highly dependent on the influent toluene concentration with broad variations. In run V the *CE* value is as high as 2275 ± 735%, which is due to the fact that a significant current was generated, even if the influent concentration of toluene was very low (i.e. 0.9 ± 0.7 mg L^{-1}). This aspect of an "impossible" *CE* will be further discussed in the following paragraphs.

The methane generation, together with the carbon capture efficiency, decreased throughout the experiment. Importantly, through all the experimental runs, the pH of the effluent was in the range 6.8–7.2 and statistically indistinguishable from the pH of the influent. This is primarily due to the fact that anode and cathode were kept in the same reaction environment, thus preventing pH unbalances (i.e. acidification of the anode and basification of the cathode) typically observed in bioelectrochemical systems employing anionic or cationic membranes

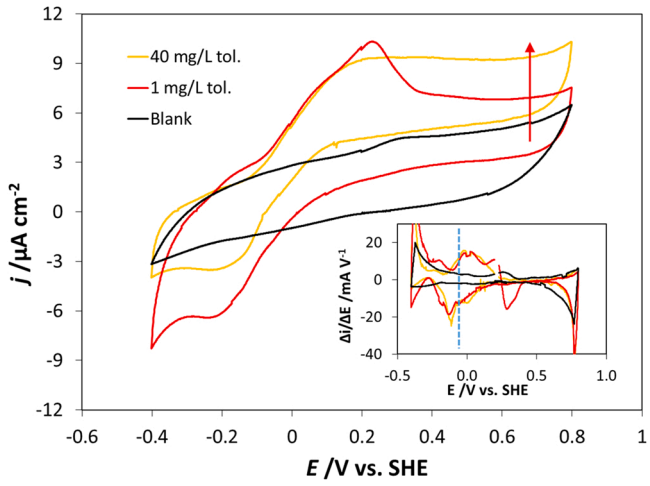

Fig. 2. Cyclic voltammograms conducted on the electrode without biofilm (abiotic control) and on the bioelectrode at two different concentrations of toluene (scan rate: 1 mV/s). The inset shows the first derivative of the voltammograms Δi/ΔE: the blue arrows point to the peaks which correspond to the formal potentials of the extracellular electron transfer of the bioelectrode.

to separate electrodic compartments.

Fig. 2 shows cyclic voltammograms (CV) recorded during different operational runs. No redox peaks were observed on the blank (abiotic) electrode either in the absence (black line) or in the presence of toluene (Fig. S2). The CV of the biofilm anode in presence of toluene (inlet toluene concentration: 1 mg L^{-1}, red line) shows a clear signal with an oxidation peak at 0.22 V vs. SHE. This strongly suggests the colonization of the electrode surface by a biofilm comprising of electroactive microorganisms, metabolically linked to toluene degradation. When the toluene concentration was increased (inlet toluene concentration: 40 mg L^{-1}, yellow line), a corresponding rise of the oxidative current is apparent, showing a clear catalytic wave, with a maximum current density of ca. 9.3 μA cm^{-2}.

By calculating the first derivative $\Delta i/\Delta E$ of the CVs of the bioanode in the presence of toluene, the formal potential (E_f) of the redox sites (directly or indirectly) involved in toluene oxidation is gained. The average E_f obtained for all feeding cycles is 0.03 ± 0.02 V vs. SHE. This value is slightly higher than the ones reported in literature for *Geobacter*-dominated anodic biofilms, which is between − 0.10 V and 0.15 V vs. SHE [34,35,41].

4.2. Impact of toluene load

The concentration of toluene in the influent had a significant impact on the reactor performance. As depicted in Fig. 3A, toluene removal rate displayed a linear dependency on the inlet toluene concentration, whereas current generation shows a non-linear relationship. Specifically, the current increase is linear at low influent toluene concentrations, while for concentrations higher than 10 mg L^{-1} the curve shows a saturation behavior (Fig. 3B). This aspect is further confirmed by the CV analysis (using CV data collected during the different runs), when plotting the value of current (at 0.7 V vs. SHE during the anodic scan of the CV) as a function of toluene concentration (Fig. 3C). Obviously, the mismatch between toluene removal and current generation trends has a major impact on the *CE*, which shows an inverse correlation with the toluene load, dropping from 134% at 5 mg L^{-1} down to 30% at 40 mg L^{-1} inlet concentration, respectively (Fig. 3D). This phenomenon seems to indicate that, at high concentrations of toluene, another route of toluene removal, which is not linked to electric current generation, becomes predominant.

Along this, it is possible that toluene is degraded under methanogenic conditions. To test this hypothesis, we conducted a run of the reactor under OCP conditions (Fig. 4), in order to quantify the contribution of the methanogenic pathway on toluene removal, upon blocking the microbial electrochemical oxidation.

However, the obtained results indicate that methane generation accounts only for a minor share of the removed toluene (Fig. 4). Indeed, the methane conversion efficiency (i.e., the percentage of the removed toluene which was recovered as methane) was as low as 7.7%. Thus methanogenic toluene degradation cannot explain the observed uncoupling between current generation and toluene removal.

4.3. Deciphering microbial syntrophy

Considering the previous results, we speculated that the degradation of toluene involves different steps in series: first toluene is converted into metabolic intermediates without the involvement of the electroactive microorganisms, subsequently these intermediates are oxidized by the electroactive bacteria in the anodic biofilm. This hypothesis was tested by performing another open circuit experiment with the reactor being operated, this time, in batch mode so as to magnify the possible accumulation of metabolic intermediates.

To this aim, the reactor was emptied to remove all metabolites and microorganisms present in the planktonic phase and then completely filled with fresh medium spiked with 10 mg L^{-1} toluene. Cyclic voltammograms were performed, at given time intervals, during the

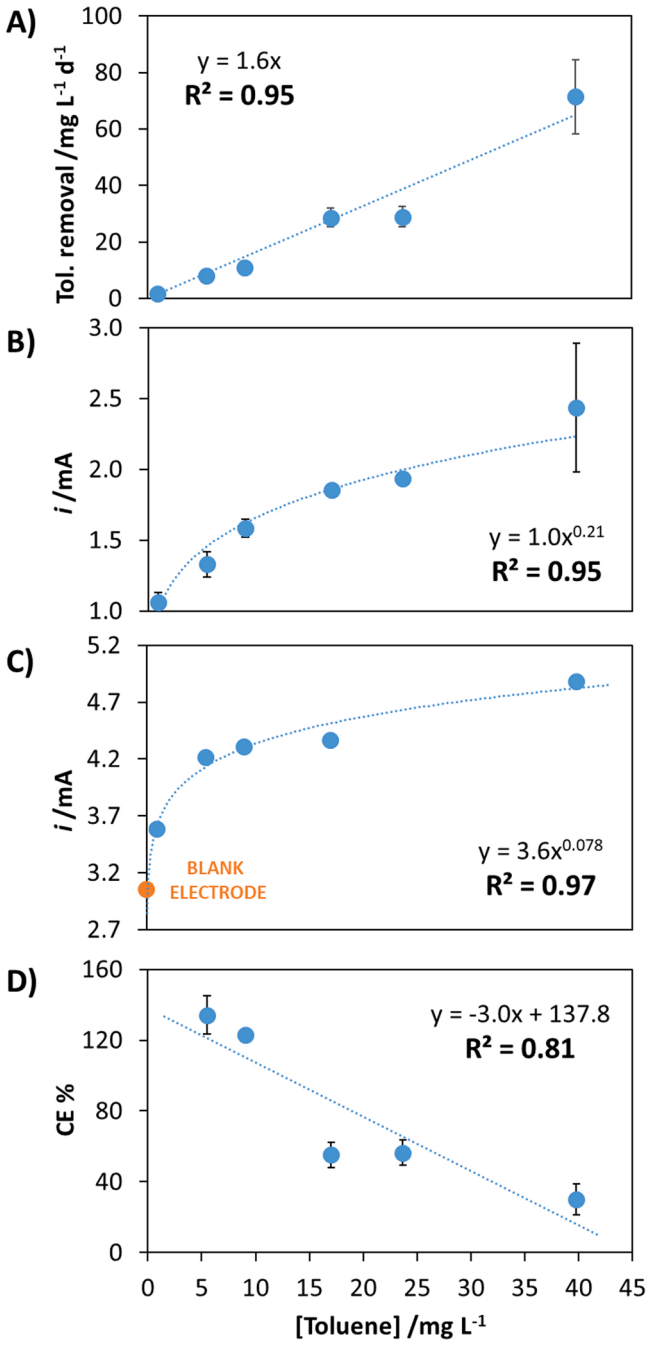

Fig. 3. Influence of the toluene concentration on A) toluene removal, B) current generation C) oxidative current obtained during CVs, in correspondence to an anodic potential of 0.7 V vs. SHE, and D) coulombic efficiency.

experiment to monitor the bioelectrocatalytic activity, while the abundance of metabolites (i.e., molecules which are directly converted into electric current by the electroactive biofilm) was quantified using NMR.

In Fig. 5 it is possible to see how, while the toluene concentration rapidly decreases, the oxidative current obtained during CVs increases, reaching a peak after about 29 h (phase I). After that the current starts decreasing again (phase II).

These results show that the microbial electrochemical activity is linked to the abundance of certain metabolites stemming from toluene degradation. They also seem to confirm that bioelectrochemical toluene degradation requires a syntrophic or cooperative interaction between different microbial populations: initially toluene is rapidly converted into metabolic intermediates (i.e. VFAs, including formate and also

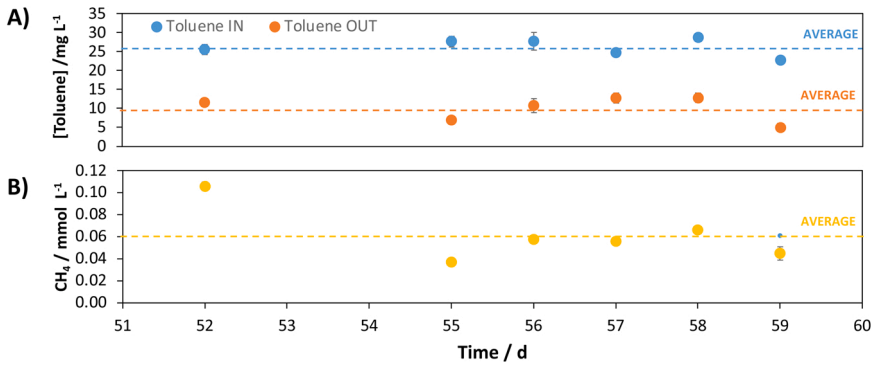

Fig. 4. Trends of toluene concentrations in the influent and effluent of the reactor and methane produced for the reactor operated in OCP mode.

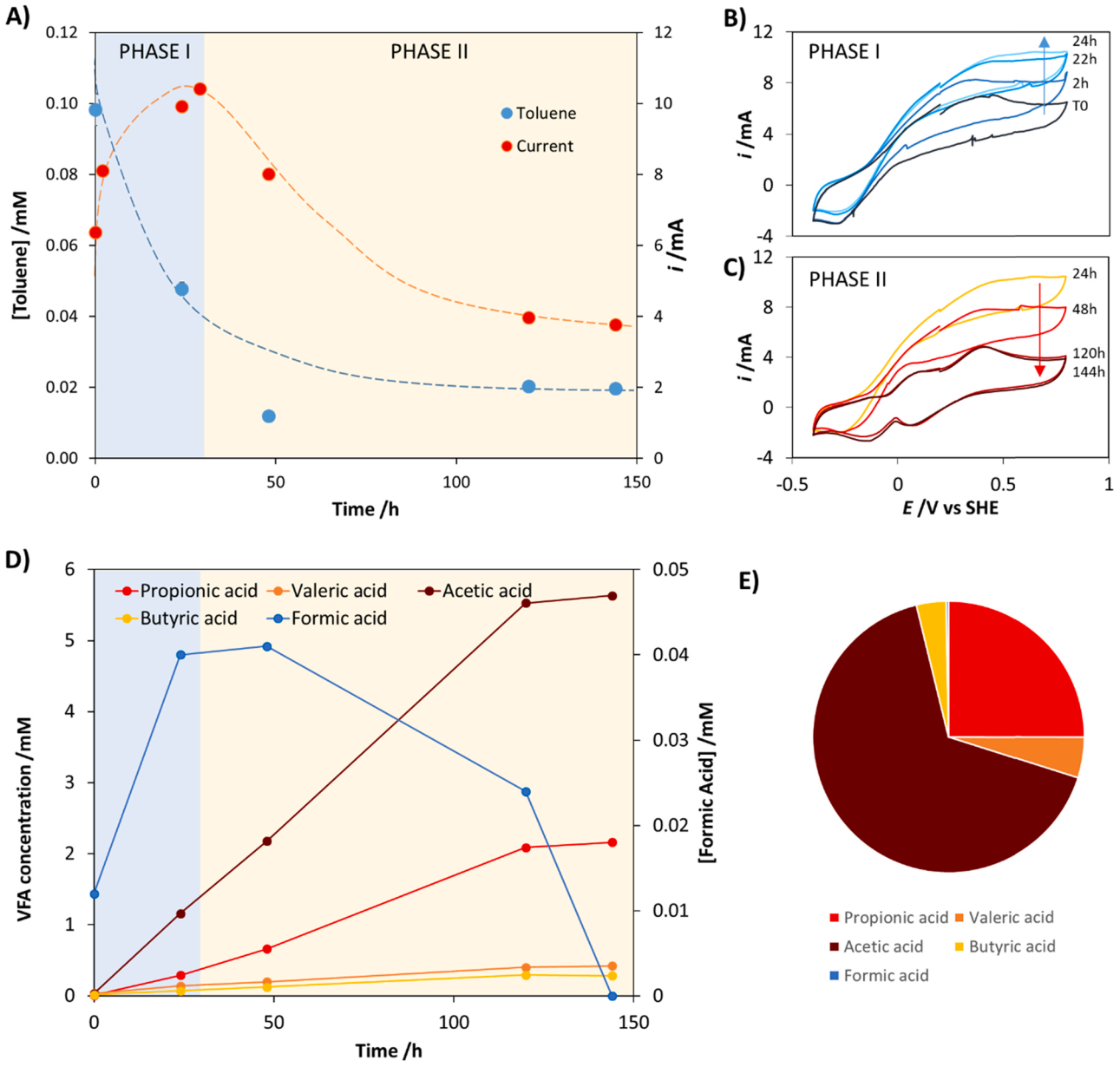

Fig. 5. A) Trend of the toluene concentration and the oxidative current recorded at 0.7 V vs. SHE during cyclic voltammograms while the reactor was operated in batch mode in OCP. B) Cyclic voltammograms recorded at different times during the step of intermediate accumulation. C) Cyclic voltammograms recorded at different times during the step of intermediate depletion. D) Trend of VFA and formic acid concentration, as determined by NMR. E) VFA composition after 150 h.

likely H_2), then the intermediates are further oxidized by electroactive bacteria present on the anode or, to a minor extent, in a methanogenic pathway in the bulk of the reactor. Therefore, VFAs are likely employed as electron carriers in a sort of metabolite cross-feeding. Indeed, VFAs are well-known substrates for electroactive microorganisms [19,20,36,54]. It can be noticed how the accumulation process in phase I is much faster than the degradation process in phase II, which explains the different behavior of toluene removal and current generation, which was mainly observed during the reactor's runs at high concentrations of toluene and under polarization. This mechanism can also explain why in run V the current was still relatively high even in absence of toluene: the metabolic intermediates present in the bulk or stored within the biofilm were still available for oxidation by the bioanode.

4.4. Microbial community features

The key functional genes involved in the anaerobic degradation of petroleum hydrocarbons were quantified using ddPCR assays. In particular, in the contaminated groundwater (T_0_bulk) the biomarkers of benzoyl-CoA desaturation (genes *bcrC, bzdN, bamB*) in the central pathway for the conversion of benzylsuccinate into acetyl-CoA [4,13] were present in the range 9.2 ^{3} gene copies L^{-1} and 3.7×10^4 gene copies L^{-1} (Fig. 6), showing a high biodegradation potential.

In line with the performances of the reactor, the abundances of the functional genes involved in toluene degradation (e.g., *bssA, brcC, bzdN, bamB*) were substantially higher in the liquid effluent sampled at the end of the reactor operation than in the groundwater used as inoculum. In particular, an enrichment of the benzylsuccinate synthase (*bssA*), a biomarker gene of anaerobic toluene degrading bacteria that use fumarate addition pathway was observed [29], with values ranged from 0 (b.d.l.) to 1.0×10^6 gene copies L^{-1}. Also, in line with the toluene degradation data, the abundance of functional genes encoding for the ATP-dependent class I (*brcC, bzdN*) and the ATP-independent class II (*bamB*) benzoyl CoA reductases were higher in the bulk at the end of the reactor operation rather than in the inoculum. In detail, the *bamB* gene accounted for 5.7×10^4 gene copies L^{-1}, *bcrC* for 1.9×10^7 gene copies L^{-1}, and *bzdN* for 2.2×10^5 gene copies L^{-1}.

The key-functional genes involved in the anaerobic toluene degradation pathway were highly abundant also in the biofilm grown on graphite rods (Fig. 6), suggesting an electroactive microbial community highly involved in this process. In particular, the *bcrC* showed the highest abundance (1.2×10^7 gene copies per cm^2 graphite), followed by *bssA* (3.7×10^4 gene copies per cm^2 graphite), *bamB* (9.0×10^3 gene copies per cm^2 graphite), and *bzdN* (3.3×10^3 gene copies per cm^2 graphite).

The microbial community analysis by means of high-throughput sequencing revealed a high diversity in both bacterial (Simpson index: 0.93, Shannon: 3.37) and archaeal (Simpson index: 0.85, Shannon: 2.12) composition in the groundwater used as inoculum of the reactor. The bacterial microbiome of the liquid phase was mainly characterized by the presence of *Betaproteobacteriales* affiliated with *Undibacterium* (12.7% of total reads), *Curvibacter* (7.3%), *Ralstonia* (4.6%), and *Rhodoferax* (3.3%) genera, followed by 18.4% of reads affiliated with family *Spirochaetaceae* (phylum *Spirochaetes*) (Fig. 7a). The phyla *Actinobacteria, Chloroflexi, Bacteroidetes*, and *Firmicutes* represented up to 34.8% of total reads. The archaeal portion of microbial community was mainly composed by *Methanocella* (16.2%), *Methanoregula* (21.4%), and *Candidatus Methanoperedens* (11.3%), followed by not identified members of *Micrarchaeia* (21.4) and *Woesearchaeia* (9.2%) classes (Fig. 7b).

At the end of the operation, a different microbial community composition was observed in the effluent. In particular, the large majority of the bacterial reads recovered by the sequencing were affiliated with the families *Propionibacteriaceae* (52.7%), *Rhodocyclaceae* (18.5%), *Rhizobiaceae* (12.0%), and *Burkholderiaceae* (2.6%). Among these families, the presence of genera *Mesorhizobium* and *Zooglea*, together with identified members of *Rhodocyclaceae* suggested high potentialities of bulk reactor microbiome in hydrocarbon degradation [2,44,45,49]. Furthermore, in line with the observed production of acetic and propionic acids [15], a large occurrence of *Propionicicella* (52.4%, Fig. 7a) was observed. The archaeal microbiome was strongly selected (Simpson index 0.07, Shannon 0.19) and mainly represented by *Methanobacterium* (96.6% of total reads) (Fig. 7b). The relative abundance of this hydrogenotrophic methanogen is in line with the CH_4 production observed in this study and consistent with previous reports on archaeal communities in methanogenic bioelectrochemical reactors [7,40,42,48].

The microbial community in the anodic biofilm grown on graphite rods provided direct evidence for the enrichment of electroactive bacteria. The classes *Anaerolineae* and *Clostridia* represented the main taxa colonizing the biofilm. Within these classes, *Anaerolineaceae*, a well-known electroactive bacterial family [12,38,52], represented up to 34.1% of total reads (Fig. 7a). Furthemore, the occurrence of several reads affiliated with genera *Geobacter and Desulfovibrio* are in line with previous evidences of these typical electroactive microorganisms in electrode biofilms [18,26]. Regarding the archaeal microbiome, also in the case of biofilm, *Methanobacterium* dominated the archaeal community representing up to 90.3% of archaeal reads (Fig. 7b).

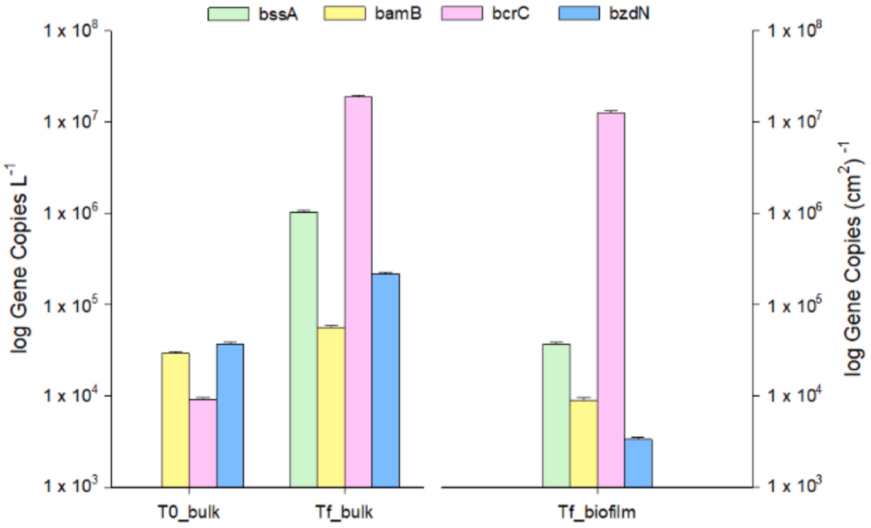

Fig. 6. Abundance of key-functional genes involved in anaerobic toluene degradation estimated by ddPCR in the liquid effluent of the reactor (T_0 and T_f) and biofilm grown on graphite rods. Data are reported in Log scale.

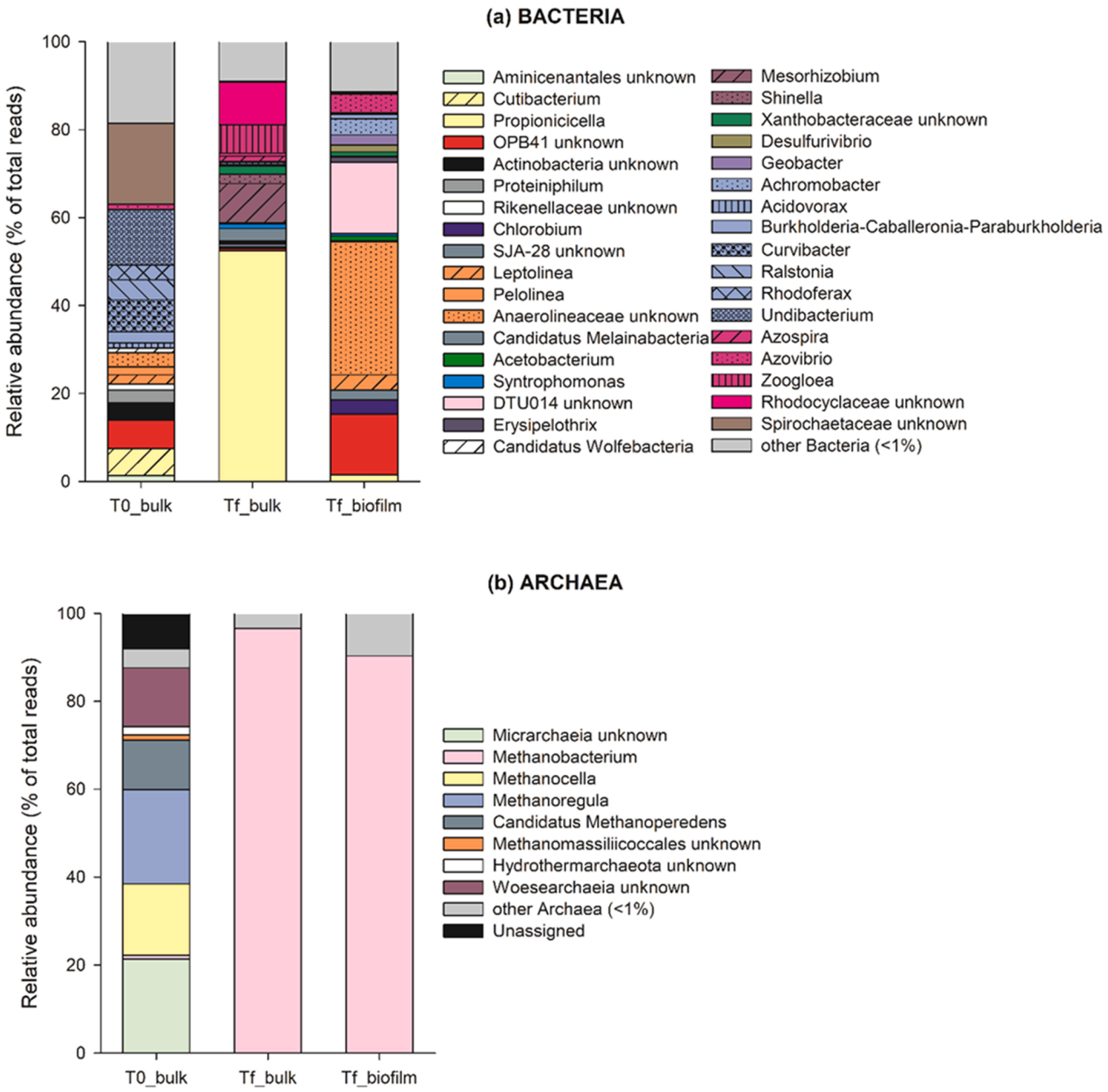

Fig. 7. Relative abundance (% of total reads) of bacterial and archaeal genera ($\geq$1% in at least one sample) in the liquid effluent of the reactor sampled at the beginning (T_0) and at the end (T_f) of the experiment and biofilm grown on graphite rods (Tf-biofilm).

Microbiological data obtained in this study suggested a close interplay and synergy between suspended (bulk) and immobilized (biofilm) biomass, in line with reactor performance (Fig. 8). Indeed, according to previous reports [2,44,45,49], the hydrocarbon degraders *Rhodocyclaceae* and *Rhizobiaceae* present in the bulk could drive the degradation of toluene leading to the production of key intermediates useful for the subsequent fermentative processes, most likely operated by *Propionicicella* members [15]. Progressively, the VFAs as well as H_2 produced by fermentation can be used by electroactive bacteria, namely *Geobacter*, *Desulfovibrio* and *Anaerolinaceae*, for generating CO_2 and H^+ [22–24,37]. At the same time, the hydrogenotrophic methanogen *Methanobacterium* can be considered responsible for the minor methane production observed in the reactor [7,40,42,48]. The microbiome described in the present study strongly supported the previous idea of a syntrophic interaction between hydrocarbon degrading bacteria, fermenters and electroactive microorganisms in bioelectrochemical systems [14,22]. Anyway, the metabolite or electron transfer between hydrocarbon degraders and methanogenic archaea is complex and not well-understood so far [10,14,22].

5. Conclusions

This study shows that the degradation of toluene to CO_2 in a bioelectrochemical system known as the “bioelectric well” is based on a syntrophic interaction between different groups of microorganisms. The degradation process involves at least two steps with different rates: in the first and faster step toluene is broken down to metabolic intermediates like VFAs by microbes able to open the aromatic ring (most probably following an initial fumarate addition). Secondly in a slower step VFAs are competitively consumed by either the electroactive biofilm on the anode or the methanogens in the bulk liquid. This mechanism explains why for higher toluene concentration the removal is

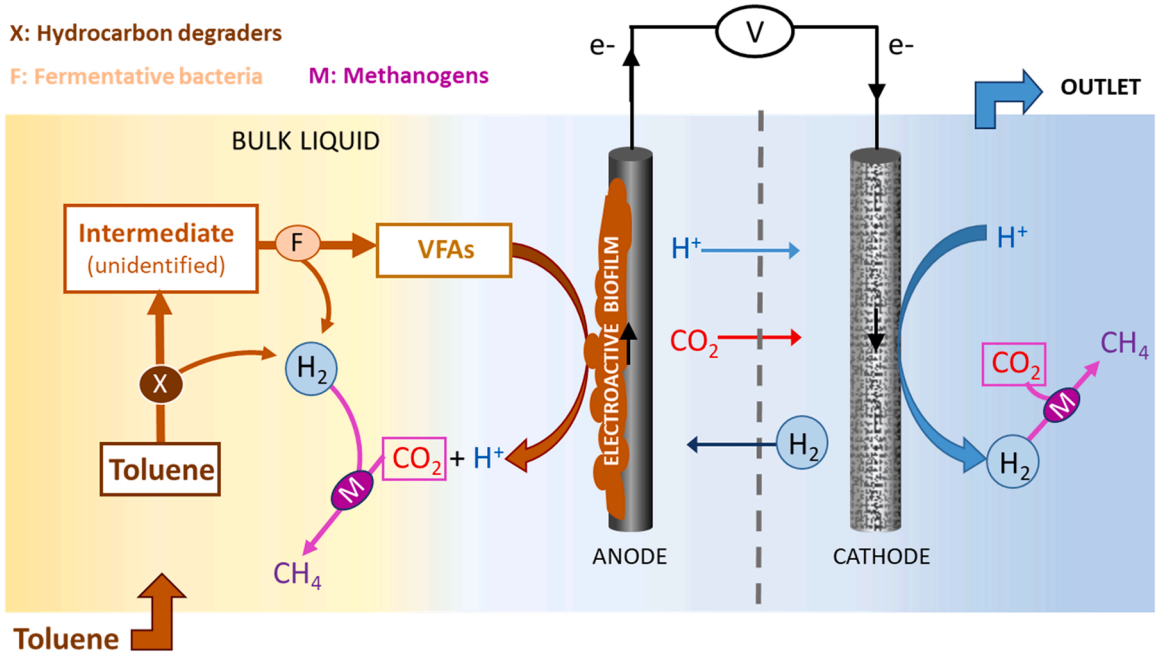

Fig. 8. Proposed mechanism for the bioelectrochemical degradation of toluene in the reactor while polarized and operated in continuous-flow mode.

linearly correlated with the toluene load, while the current generation tends to a plateau, causing a decrease of the columbic efficiency. Indeed, the metabolic intermediates accumulate in the reactor or are stored in the biofilm, causing current generation even in absence of the only carbon source (i.e. toluene).

These findings highlight the importance of a diverse microbial environment for the successful bioelectrochemical degradation of recalcitrant pollutants such as aromatic petroleum hydrocarbons. Additionally, the bioelectric well prototype proved to be an interesting tool to investigate the biodegradation pathways of organic contaminants, thanks to the combination of chemical, electrochemical and biomolecular analyses. The absence of a membrane separating anodic and cathodic compartments allowed to gather insights on the complex interplay between the different microbial populations and electrodes. This study further paves the way for the successful design and implementation of bioelectrochemical technologies applicable either in-situ or *on site*.

Future research should focus on fine-tuning the reactor architecture and microbial and operational characteristic of the bioelectric well in order to optimize the removal efficiency and rate, especially in real environments.

CRediT authorship contribution statement

Matteo Tucci: Conceptualization, Methodology, Formal analysis, Data curation, Writing – original draft. **Alessandro Milani:** Investigation, Data curation. **Marco Resitano:** Investigation, Data curation. **Carolina Cruz Viggi:** Conceptualization, Methodology, Formal analysis, Data curation, Writing – original draft. **Ottavia Giampaoli:** Investigation, Formal analysis, Writing – original draft. **Alfredo Miccheli:** Investigation, Formal analysis, Writing – original draft. **Simona Crognale:** Conceptualization, Methodology, Formal analysis, Data curation, Writing – original draft. **Bruna Matturro:** Conceptualization, Methodology, Formal analysis. **Simona Rossetti:** Conceptualization, Methodology, Formal analysis. **Falk Harnisch:** Conceptualization, Methodology, Writing – original draft. **Federico Aulenta:** Conceptualization, Resources, Writing – review & editing.

Declaration of Competing Interest

The authors declare that they have no known competing financial interests or personal relationships that could have appeared to influence the work reported in this paper.

Aknowledgements

This study was supported by the European Union's Horizon 2020 project ELECTRA (www.electra.site) under grant agreement No. 826244.

Appendix A. Supporting information

Supplementary data associated with this article can be found in the online version at doi:10.1016/j.jece.2022.107799.

References

[1] I. Akmirza, C. Pascual, A. Carvajal, R. Pérez, R. Muñoz, R. Lebrero, Anoxic biodegradation of BTEX in a biotrickling filter, Sci. Total Environ. 587–588 (2017) 457–465, https://doi.org/10.1016/j.scitotenv.2017.02.130.

[2] H.P. Bacosa, J. Steichen, M. Kamalanathan, R. Windham, A. Lubguban, J. M. Labonté, K. Kaiser, D. Hala, P.H. Santschi, A. Quigg, Polycyclic aromatic hydrocarbons (PAHs) and putative PAH-degrading bacteria in Galveston Bay, TX (USA), following Hurricane Harvey (2017), Environ. Sci. Pollut. Res. 27 (2020) 34987–34999, https://doi.org/10.1007/s11356-020-09754-5.

[3] A.L. Bolden, C.F. Kwiatkowski, T. Colborn, New look at BTEX: are ambient levels a problem, Environ. Sci. Technol. 49 (2015) 5261–5276, https://doi.org/10.1021/es505316f.

[4] M. Boll, C. Löffler, B.E.L. Morris, J.W. Kung, Anaerobic degradation of homocyclic aromatic compounds via arylcarboxyl-coenzyme A esters: organisms, strategies and key enzymes, Environ. Microbiol. 16 (2014) 612–627, https://doi.org/10.1111/1462-2920.12328.

[5] E. Bolyen, J.R. Rideout, M.R. Dillon, N.A. Bokulich, C.C. Abnet, G.A. Al-Ghalith, H. Alexander, E.J. Alm, M. Arumugam, F. Asnicar, Y. Bai, J.E. Bisanz, K. Bittinger, A. Brejnrod, C.J. Brislawn, C.T. Brown, B.J. Callahan, A.M. Caraballo-Rodríguez, J. Chase, E.K. Cope, R. Da Silva, C. Diener, P.C. Dorrestein, G.M. Douglas, D. M. Durall, C. Duvallet, C.F. Edwardson, M. Ernst, M. Estaki, J. Fouquier, J. M. Gauglitz, S.M. Gibbons, D.L. Gibson, A. Gonzalez, K. Gorlick, J. Guo, B. Hillmann, S. Holmes, H. Holste, C. Huttenhower, G.A. Huttley, S. Janssen, A. K. Jarmusch, L. Jiang, B.D. Kaehler, K. Kang, Bin, C.R. Keefe, P. Keim, S.T. Kelley, D. Knights, I. Koester, T. Kosciolek, J. Kreps, M.G.I. Langille, J. Lee, R. Ley, Y. X. Liu, E. Loftfield, C. Lozupone, M. Maher, C. Marotz, B.D. Martin, D. McDonald, L. J. McIver, A.V. Melnik, J.L. Metcalf, S.C. Morgan, J.T. Morton, A.T. Naimey, J. A. Navas-Molina, L.F. Nothias, S.B. Orchanian, T. Pearson, S.L. Peoples, D. Petras,

M.L. Preuss, E. Pruesse, L.B. Rasmussen, A. Rivers, M.S. Robeson, P. Rosenthal, N. Segata, M. Shaffer, A. Shiffer, R. Sinha, S.J. Song, J.R. Spear, A.D. Swafford, L. R. Thompson, P.J. Torres, P. Trinh, A. Tripathi, P.J. Turnbaugh, S. Ul-Hasan, J.J. J. van der Hooft, F. Vargas, Y. Vázquez-Baeza, E. Vogtmann, M. von Hippel, W. Walters, Y. Wan, M. Wang, J. Warren, K.C. Weber, C.H.D. Williamson, A. D. Willis, Z.Z. Xu, J.R. Zaneveld, Y. Zhang, Q. Zhu, R. Knight, J.G. Caporaso, Reproducible, interactive, scalable and extensible microbiome data science using QIIME 2, Nat. Biotechnol. 37 (2019) 852–857, https://doi.org/10.1038/s41587-019-0209-9.

[6] D. Cecconet, F. Sabba, M. Devecseri, A. Callegari, A.G. Capodaglio, In situ groundwater remediation with bioelectrochemical systems: a critical review and future perspectives, Environ. Int. 137 (2020), 105550, https://doi.org/10.1016/j.envint.2020.105550.

[7] S. Cheng, D. Xing, D. Call, B. Logan, Direct biological conversion of electrical current into methane by electromethanogenesis, Environ. Sci. Technol. 43 (2009) 3953–3958.

[8] S. Crognale, C.M. Braguglia, A. Gallipoli, A. Gianico, S. Rossetti, D. Montecchio, Direct conversion of food waste extract into caproate: metagenomics assessment of chain elongation process, Microorganisms (2021) 9, https://doi.org/10.3390/microorganisms9020327.

[9] S. Crognale, B. Casentini, S. Amalfitano, S. Fazi, M. Petruccioli, S. Rossetti, Biological As(III) oxidation in biofilters by using native groundwater microorganisms, Sci. Total Environ. (2019) 651, https://doi.org/10.1016/j.scitotenv.2018.09.176.

[10] M. Embree, H. Nagarajan, N. Movahedi, H. Chitsaz, K. Zengler, Single-cell genome and metatranscriptome sequencing reveal metabolic interactions of an alkane-degrading methanogenic community, ISME J. 8 (2014) 757–767, https://doi.org/10.1038/ismej.2013.187.

[11] M. Farhadian, C. Vachelard, D. Duchez, C. Larroche, In situ bioremediation of monoaromatic pollutants in groundwater: a review, Bioresour. Technol. 99 (2008) 5296–5308, https://doi.org/10.1016/j.biortech.2007.10.025.

[12] Q. Feng, Y.C. Song, J. Li, Z. Wang, Q. Wu, Influence of electrostatic field and conductive material on the direct interspecies electron transfer for methane production, Environ. Res. 188 (2020), 109867, https://doi.org/10.1016/j.envres.2020.109867.

[13] G. Fuchs, M. Boll, J. Heider, Microbial degradation of aromatic compounds- from one strategy to four, Nat. Rev. Microbiol. 9 (2011) 803–816, https://doi.org/10.1038/nrmicro2652.

[14] L.M. Gieg, S.J. Fowler, C. Berdugo-Clavijo, Syntrophic biodegradation of hydrocarbon contaminants, Curr. Opin. Biotechnol. 27 (2014) 21–29, https://doi.org/10.1016/j.copbio.2013.09.002.

[15] M. Goodfellow, P. Kampfer, H.-J. Busse, M.E. Trujillo, K. Suzuki, W. Ludwig, W. B. Whitman, The actinobacteria, in: Bergey's Manual of Systematic Bacteriology, 2012.

[16] Ø. Hammer, D.A.T.A.T. Harper, P.D. Ryan, PAST: paleontological statistics software package for education and data analysis, Palaeontol. Electron. 4 (1) (2001) 1–9, https://doi.org/10.1016/j.bcp.2008.05.025.

[17] Y.T. He, C. Su, Use of additives in bioremediation of contaminated groundwater and soil, Adv. Bioremediat. Wastewater Polluted Soil (2015) 145–164, https://doi.org/10.1016/j.colsurfa.2011.12.014.

[18] R. Hou, L. Gan, F. Guan, Y. Wang, J. Li, S. Zhou, Y. Yuan, Bioelectrochemically enhanced degradation of bisphenol S: mechanistic insights from stable isotope-assisted investigations, iScience (2021) 24, https://doi.org/10.1016/j.isci.2020.102014.

[19] X. Jin, I. Angelidaki, Y. Zhang, Microbial electrochemical monitoring of volatile fatty acids during anaerobic digestion, Environ. Sci. Technol. 50 (2016) 4422–4429, https://doi.org/10.1021/acs.est.5b05267.

[20] P.D. Kiely, J.M. Regan, B.E. Logan, The electric picnic: synergistic requirements for exoelectrogenic microbial communities, Curr. Opin. Biotechnol. 22 (2011) 378–385, https://doi.org/10.1016/j.copbio.2011.03.003.

[21] K. Kuntze, C. Vogt, C. Richnow, H.H. Boll, M, Combined application of PCR-based functional assays for the detection of aromatic-compound-degrading anaerobes, Appl. Environ. Microbiol. 77 (2011) 5056–5061, https://doi.org/10.1128/AEM.00335-11.

[22] K. Laczi, Á. Erdeiné Kis, Á. Szilágyi, N. Bounedjoum, A. Bodor, G.E. Vincze, T. Kovács, G. Rákhely, K. Perei, New frontiers of anaerobic hydrocarbon biodegradation in the multi-omics era, Front. Microbiol. 11 (2020) 1–20, https://doi.org/10.3389/fmicb.2020.590049.

[23] B. Liang, L.Y. Wang, S.M. Mbadinga, J.F. Liu, S.Z. Yang, J.D. Gu, B.Z. Mu, Anaerolineaceae and Methanosaeta turned to be the dominant microorganisms in alkanes-dependent methanogenic culture after long-term of incubation, AMB Express (2015) 5, https://doi.org/10.1186/s13568-015-0117-4.

[24] B. Liang, L.Y. Wang, Z. Zhou, S.M. Mbadinga, L. Zhou, J.F. Liu, S.Z. Yang, J.D. Gu, B.Z. Mu, High frequency of thermodesulfovibrio spp. and Anaerolineaceae in association with methanoculleus spp. in a long-term incubation of n-alkanes-degrading methanogenic enrichment culture, Front. Microbiol. 7 (2016) 1–13, https://doi.org/10.3389/fmicb.2016.01431.

[25] C. Löffler, K. Kuntze, J.R. Vazquez, A. Rugor, J.W. Kung, A. Böttcher, M. Boll, Occurrence, genes and expression of the W/Se-containing class II benzoyl-coenzyme A reductases in anaerobic bacteria, Environ. Microbiol. 13 (2011) 696–709, https://doi.org/10.1111/j.1462-2920.2010.02374.x.

[26] D.R. Lovley, Live wires: direct extracellular electron exchange for bioenergy and the bioremediation of energy-related contamination, Energy Environ. Sci. 4 (2011) 4896–4906, https://doi.org/10.1039/c1ee02229f.

[27] M. Mehrjouei, S. Müller, D. Möller, Energy consumption of three different advanced oxidation methods for water treatment: a cost-effectiveness study, J. Clean. Prod. 65 (2014) 178–183, https://doi.org/10.1016/j.jclepro.2013.07.036.

[28] O. Modin, F. Aulenta, Three promising applications of microbial electrochemistry for the water sector, Environ. Sci. Water Res. Technol. 3 (2017) 391–402, https://doi.org/10.1039/c6ew00325g.

[29] F.Von Netzer, C. Vogt, H. Richnow, Functional gene markers for fumarate-adding and dearomatizing key enzymes in anaerobic aromatic hydrocarbon degradation in terrestrial environments, J. Mol. Microbiol. Biotechnol. (2016) 180–194, https://doi.org/10.1159/000441946.

[30] E. Okoh, Z.R. Yelebe, B. Oruabena, E.S. Nelson, O.P. Indiamaowei, Clean-up of crude oil-contaminated soils: bioremediation option, Int. J. Environ. Sci. Technol. 17 (2020) 1185–1198, https://doi.org/10.1007/s13762-019-02605-y.

[31] E. Palma, M. Daghio, A. Espinoza Tofalos, A. Franzetti, C. Cruz Viggi, S. Fazi, M. Petrangeli Papini, F. Aulenta, Anaerobic electrogenic oxidation of toluene in a continuous-flow bioelectrochemical reactor: process performance, microbial community analysis, and biodegradation pathways, Environ. Sci. Water Res. Technol. 4 (2018) 2136–2145, https://doi.org/10.1039/c8ew00666k.

[32] E. Palma, M. Daghio, A. Franzetti, M. Petrangeli Papini, F. Aulenta, The bioelectric well: a novel approach for in situ treatment of hydrocarbon-contaminated groundwater, Microb. Biotechnol. 11 (2018) 112–118, https://doi.org/10.1111/1751-7915.12760.

[33] E. Palma, A. Espinoza Tofalos, M. Daghio, A. Franzetti, P. Tsiota, C. Cruz Viggi, M. P.M.P. Papini, F. Aulenta, Bioelectrochemical treatment of groundwater containing BTEX in a continuous-flow system: substrate interactions, microbial community analysis, and impact of sulfate as a co-contaminant, New Biotechnol. 53 (2019) 41–48, https://doi.org/10.1016/j.nbt.2019.06.004.

[34] S.A. Patil, C. Hägerhäll, L. Gorton, Electron transfer mechanisms between microorganisms and electrodes in bioelectrochemical systems, Bioanal. Rev. 4 (2012) 159–192, https://doi.org/10.1007/s12566-012-0033-x.

[35] S. Riedl, R. Brown, D. Alvarez Esquivel, H. Wichmann, K. Huber, B. Bunk, J. Overmann, U. Schröder, Cultivating electrochemically active biofilms at continuously changing electrode potentials, ChemElectroChem 6 (2019) 2238–2247, https://doi.org/10.1002/celc.201900036.

[36] A. Rosales-Sierra, S. Rosales-Mendoza, E. Monreal-Escalante, L.B. Celis, E. Razo-Flores, B. Cercado, Acclimation strategy using complex volatile fatty acid mixtures increases the microbial fuel cell (MFC) potential, ChemistrySelect 2 (2017) 6277–6285, https://doi.org/10.1002/slct.201701267.

[37] K. Rossmassler, C.D. Snow, D. Taggart, C. Brown, S.K. De Long, Advancing biomarkers for anaerobic o-xylene biodegradation via metagenomic analysis of a methanogenic consortium, Appl. Microbiol. Biotechnol. 103 (2019) 4177–4192, https://doi.org/10.1007/s00253-019-09762-7.

[38] P. Roustazadeh Sheikhyousefi, M. Nasr Esfahany, A. Colombo, A. Franzetti, S. P. Trasatti, P. Cristiani, Investigation of different configurations of microbial fuel cells for the treatment of oilfield produced water, Appl. Energy 192 (2017) 457–465, https://doi.org/10.1016/j.apenergy.2016.10.057.

[39] R. Sander, Compilation of Henry's law constants (version 4.0) for water as solvent, Atmos. Chem. Phys. 15 (2015) 4399–4981, https://doi.org/10.5194/acp-15-4399-2015.

[40] K. Sasaki, M. Morita, D. Sasaki, S. ichi Hirano, N. Matsumoto, N. Ohmura, Y. Igarashi, Methanogenic communities on the electrodes of bioelectrochemical reactors without membranes, J. Biosci. Bioeng. 111 (2011) 47–49, https://doi.org/10.1016/j.jbiosc.2010.08.010.

[41] F. Scarabotti, L. Rago, K. Bühler, F. Harnisch, The electrode potential determines the yield coefficients of early-stage Geobacter sulfurreducens biofilm anodes, Bioelectrochemistry 140 (2021), 107752, https://doi.org/10.1016/j.bioelechem.2021.107752.

[42] M. Siegert, X.F. Li, M.D. Yates, B.E. Logan, The presence of hydrogenotrophic methanogens in the inoculum improves methane gas production in microbial electrolysis cells, Front. Microbiol. 5 (2014) 1–12, https://doi.org/10.3389/fmicb.2014.00778.

[43] M.P. Suarez, H.S. Rifai, Evaluation of BTEX remediation by natural attenuation at a coastal facility, Gr. Water Monit. Remed. 22 (2002) 62–77.

[44] A. Táncsics, M. Farkas, B. Horváth, G. Maróti, L.M. Bradford, T. Lueders, B. Kriszt, Genome analysis provides insights into microaerobic toluene-degradation pathway of Zoogloea oleivorans BucT, Arch. Microbiol. 202 (2020) 421–426, https://doi.org/10.1007/s00203-019-01743-8.

[45] A. Táncsics, A.R. Szalay, M. Farkas, T. Benedek, S. Szoboszlay, I. Szabó, T. Lueders, Stable isotope probing of hypoxic toluene degradation at the Siklós aquifer reveals prominent role of Rhodocyclaceae, FEMS Microbiol. Ecol. 94 (2018), https://doi.org/10.1093/femsec/fiy088 fiy088.

[46] M. Tucci, C. Cruz Viggi, A. Esteve Núñez, A. Schievano, K. Rabaey, F. Aulenta, Empowering electroactive microorganisms for soil remediation: challenges in the bioelectrochemical removal of petroleum hydrocarbons, Chem. Eng. J. 419 (2021), 130008, https://doi.org/10.1016/j.cej.2021.130008.

[47] M. Tucci, C. Cruz Viggi, M. Resitano, B. Matturro, S. Crognale, I. Pietrini, S. Rossetti, F. Harnisch, F. Aulenta, Simultaneous removal of hydrocarbons and sulfate from groundwater using a "bioelectric well, Electrochim. Acta 388 (2021), 138636, https://doi.org/10.1016/j.electacta.2021.138636.

[48] M.C.A.A. Van Eerten-Jansen, A.B. Veldhoen, C.M. Plugge, A.J.M. Stams, C.J. N. Buisman, A. Ter Heijne, Microbial community analysis of a methane-producing biocathode in a bioelectrochemical system, Archaea (2013) 2013, https://doi.org/10.1155/2013/481784.

[49] S.A.B. Weelink, N.C.G. Tan, H. ten Broeke, W. van Doesburg, A.A.M. Langenhoff, J. Gerritse, A.J.M. Stams, Physiological and phylogenetic characterization of a stable benzene-degrading, chlorate-reducing microbial community, FEMS

Microbiol. Ecol. 60 (2007) 312–321, https://doi.org/10.1111/j.1574-6941.2007.00289.x.
[50] S.A.B. Weelink, M.H.A. van Eekert, A.J.M. Stams, Degradation of BTEX by anaerobic bacteria: physiology and application, Rev. Environ. Sci. Bio/Technol. 2010 (94 9) (2010) 359–385, https://doi.org/10.1007/S11157-010-9219-2.
[51] C. Winderl, S. Schaefer, T. Lueders, Detection of anaerobic toluene and hydrocarbon degraders in contaminated aquifers using benzylsuccinate synthase (bssA) genes as a functional marker, Environ. Microbiol. 9 (2007) 1035–1046, https://doi.org/10.1111/j.1462-2920.2006.01230.x.
[52] H. Xu, C. Wang, K. Yan, J. Wu, J. Zuo, K. Wang, Anaerobic granule-based biofilms formation reduces propionate accumulation under high H2 partial pressure using conductive carbon felt particles, Bioresour. Technol. 216 (2016) 677–683, https://doi.org/10.1016/j.biortech.2016.06.010.
[53] K. Yang, M. Ji, B. Liang, Y. Zhao, S. Zhai, Z. Ma, Z. Yang, Bioelectrochemical degradation of monoaromatic compounds: current advances and challenges, J. Hazard. Mater. 398 (2020), 122892, https://doi.org/10.1016/J.JHAZMAT.2020.122892.
[54] Z. Zhang, J. Li, X. Hao, Z. Gu, S. Xia, Electron donation characteristics and interplays of major volatile fatty acids from anaerobically fermented organic matters in bioelectrochemical systems, Environ. Technol. 40 (2019) 2337–2344, https://doi.org/10.1080/09593330.2018.1441334.